Optical Observations of Acoustical Radiation Force Effects on Individual Air Bubbles

Peggy Palanchon, Piero Tortoli, *Senior Member, IEEE*, Ayache Bouakaz, Michel Versluis, and Nico de Jong, *Associate Member, IEEE*

***Abstract*—Previous studies dealing with contrast agent microbubbles have demonstrated that ultrasound (US) can significantly influence the movement of microbubbles. In this paper, we investigated the influence of the acoustic radiation force on individual air bubbles using high-speed photography. We emphasize the effects of the US parameters (pulse length, acoustic pressure) on different bubble patterns and their consequences on the translational motion of the bubbles. A stream of uniform air bubbles with diameter ranging from 35 μm to 79 μm was generated and insonified with a single US pulse emitted at a frequency of 130 kHz. The bubble sizes have been chosen to be above, below, and at resonance. The peak acoustic pressures used in these experiments ranged from 40 kPa to 120 kPa. The axial displacements of the bubbles produced by the action of the US pulse were optically recorded using a high-speed camera at 1 kHz frame rate. The experimental results were compared to a simplified force balance theoretical model, including the action of the primary radiation force and the fluid drag force. Although the model is quite simple and does not take into account phenomena like bubble shape oscillations and added mass, the experimental findings agree with the predictions. The measured axial displacement increases quasilinearly with the burst length and the transmitted acoustic pressure. The axial displacement varies with the size and the density of the air bubbles, reaching a maximum at the resonance size of 48 μm. The predicted displacement values differ by 15% from the measured data, except for resonant bubbles for which the displacement was overestimated by about 40%. This study demonstrates that even a single US pulse produces radiation forces that are strong enough to affect the bubble position.**

I. Introduction

In order to obtain the desired response to ultrasound (US) by microbubbles, it is necessary to know their reaction to the different forces they experience during insonation. Among these forces, the primary, or Bjerknes, radiation force [1] may play an important part in applications including targeted drug and gene delivery. Appropriate control of primary (and secondary) radiation force can in fact allow optimal assimilation of drugs into cells. Indeed cell membrane fusion with external molecules and or endocytosis mechanisms are suspected to be one of the causes of increased cell uptake and, therefore, can be amplified by a thorough understanding of the interaction between microbubbles and ultrasound radiation forces. To a lesser extent, the effect of radiation force may have been experienced in studies dealing with microemboli detection. Smith *et al.* [2] reported that Doppler embolic signals from gaseous emboli often display regions of frequency modulations, but signals originated from solid emboli never exhibits such a behavior. The reason for this sudden frequency change was not really understood; but it could be related to the displacement induced by the ultrasound waves. Further investigations are required to fully establish the influence of the radiation force on the microembolic Doppler signals.

A preliminary evaluation of radiation force effects on microbubbles has been reported by Dayton *et al.* [3], where it was optically observed that a streamline of Albunex® and MP1950 (Mallinckrodt Inc., St. Louis, MO) microbubbles was pushed away from the insonifying transducer. Experimental results have shown that, when such translations are related to full populations of contrast agents suspended in moving fluids, they may yield to considerable distortions in the corresponding Doppler spectra [4], [5]. A Doppler approach was used to indirectly validate a simple theoretical model, in which the microbubble movements are evaluated through the combination of the primary US force with the drag force of the fluid in which they are suspended. Experimental spectra obtained by insonifying full populations of Levovist© microbubbles were positively compared with the spectra estimated according to such a model [4]. A similar, but more accurate model was proposed in [6]. This model, which includes the added mass force and evaluates all the effects of bubble oscillations, was compared to experiments performed on individual MP1950 phospholipid shelled microbubbles. This paper evaluates quantitatively the influence of radiation force associated to a single US pulse on a stream of individual air bubbles with a diameter ranging from 35 μm to 79 μm. The axial displacement was measured using a high-speed imaging system. The influence of the acoustic parameters as well as of the size and the number density of the bubbles was investigated. In Section II, the experimental setup is described and the used US settings are given. Afterward, a simple simulation

Manuscript received March 10, 2004; accepted July 30, 2004. This work was supported by the European Union grant QLG1-CT-2002-01518 (UMEDS Project), and by the Italian Ministry of Education, University and Research (COFIN 2002).

P. Palanchon, A. Bouakaz, and N. de Jong are with Erasmus Medical Center, Experimental Echocardiology, Rotterdam, The Netherlands (e-mail: p.palanchon@erasmusmc.nl).

P. Palanchon is also with Erasmus Medical Center, Department of Anesthesiology, Rotterdam, The Netherlands.

P. Tortoli is with the University of Florence, Department of Electronics and Telecommunications, Florence, Italy.

A. Bouakaz and N. de Jong are also with the Interuniversity Cardiology Institute of the Netherlands, The Netherlands.

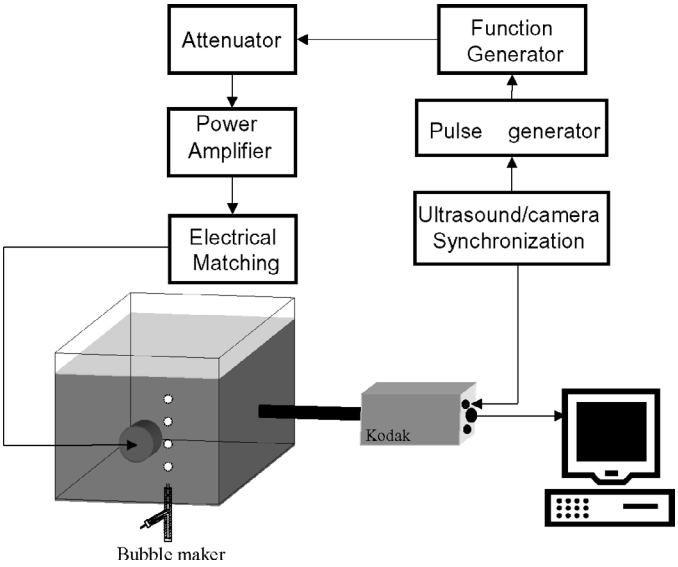

Fig. 1. Experimental setup.

model derived from the one introduced in [4] is reported, and the expressions of the primary radiation force and the drag force are presented. In Section III, the experimental results are presented and compared to simulation results. Then, possible reasons for discrepancies found around resonance are discussed.

II. Materials and Methods

A. Experimental Setup

The experimental setup is shown in Fig. 1. A streamline of bubbles was generated by a homemade bubble maker, allowing the production of calibrated and uniform air bubbles. The operator could independently control the size and the number of the generated bubbles by varying the settings of the bubble maker [7]. The bubble streamline was directed from the bottom to the top of the tank, as the bubbles are dragged by the movement of the flow generated by a gear pump. A single-element US transducer was positioned to produce acoustic waves directed perpendicularly to the streamline. The imaging system was composed of a high-speed camera (CR2000, Kodak, Vianen, The Netherlands) directly mounted on a long zoom microscope (Sciencescope, Chino, CA) and focused on the microbubbles. The frame rate of the camera was fixed at 1 kHz. A constant light source provided the necessary illumination for the recordings. The optical resolution of this system was 3 μm/pixel. The ultrasonic arrangement included a function generator producing a single sinusoidal burst, coherent with the camera frame synchronism and a radiofrequency power amplifier (Model 2100L, ENI, Rochester, MA). A homemade electrical matching circuit was used to compensate the impedance mismatch between the US transducer and the electronics. The acoustic pressure produced by the transducer could be adjusted with appropriate attenuators and was separately measured using a calibrated hydrophone (Reson GmbH, Kiel, Germany). The tip of the needle was positioned in the optical field of view, so that the measured acoustic pressure (ranging from 40 kPa to 120 kPa) corresponded to the pressure applied to the bubbles. The images taken by the high-speed camera were saved on a personal computer for analysis. The bubbles' characteristics (diameter and separation distance between two successive bubbles) as well as their displacements were computed using a MATLAB program (The Mathworks, Natick, MA).

B. Simulation Model

The displacement of the bubbles is predicted using a simple theoretical model similar to the one described by Tortoli *et al.* [4]. It assumes that the bubble displacement is induced by the action of the primary radiation force and the drag force of the fluid. The trajectory of the bubbles can be traced by solving the following vector motion equation:

$$\vec{F_{US}}(t) + \vec{F_D}(t) = m\frac{d\vec{V_b}(t)}{dt}, \tag{1}$$

where $\vec{F_{US}}$ is the primary radiation force, $\vec{F_D}$ is the drag force, $\vec{V_b}$ is the instantaneous bubble velocity, and m is the bubble mass.

The expression of the primary radiation force is similar to the one described by Dayton *et al.* [3] and Leighton [8]. It assumes that the bubble diameter is much smaller than the acoustic wavelength, the bubble remains spherically symmetric during pressure changes, and the acoustic waves are planar and parallel. When a single pulse is considered, the amplitude of the primary radiation force is expressed by:

$$\vec{F_{US}} = \frac{P_A^2 D}{2\rho c f}\frac{\delta_{tot} f_0/f}{\left[(f_0/f)^2-1\right]^2 + (\delta_{tot} f_0/f)^2}, \tag{2}$$

where f is the transmitted frequency, c is the US propagation speed, P_A is the peak acoustic pressure, f_0 is the resonance frequency, D is the equilibrium bubble diameter, ρ is the fluid density, and δ_{tot} is the total damping coefficient.

The total damping coefficient is defined by:

$$\delta_{tot} = \delta_{rad} + \delta_{vis} + \delta_{th}, \tag{3}$$

where δ_{rad}, δ_{vis}, and δ_{th} are, respectively, the damping coefficients due to the radiation, the viscosity of the surrounding medium, and the heat conduction. The expressions of these damping coefficients are given by Medwin [9].The resonance frequency was computed using the formula given by Medwin [9]:

$$f_r^2 = \frac{S_A}{4\pi^2 m} b\beta, \tag{4}$$

where S_A is the stiffness of the bubble-liquid interface, m is the effective mass of the system, $b = 1/\kappa$, κ is the polytropic exponent, and β is the surface tension.

The effective mass, the polytropic exponent, and the surface tension also were given by Medwin [9]. When an US pulse is applied to a moving bubble, it induces an acceleration of the bubble so that it is diverted from the flow path. The difference between the fluid and the bubble velocity yields to a drag force. Assuming that the bubble remains spherical and the surrounding fluid is Newtonian, the drag force is defined by the formula:

$$\vec{F_D} = C_D Re \frac{\pi D \nu \rho_0}{8} (\vec{V_f} - \vec{V_b}), \tag{5}$$

where $\vec{V_b}$ is the instantaneous bubble velocity, $\vec{V_f}$ is the fluid velocity, Re is the Reynolds number, C_D is the drag coefficient, ρ is the fluid density, and ν is the fluid viscosity.

Note that (5) does not include the effects of bubble radial motion in the translating bubbles, nor the initial acceleration of the bubble. For the experimental conditions used in this paper, the maximum Re has been estimated to be low enough to make the unsteady effects negligible.

In practice, according to this model, it is expected that each bubble is accelerated along the transducer (horizontal) axial direction until it reaches a steady velocity, V_b, such that the corresponding drag force, as described by (3), perfectly balances the radiation force. This equilibrium condition is achieved quite rapidly, and holds as long as the bubble is insonated by the US burst, i.e., for a time, T_X, depending on the transmitted burst length. At the end of such time interval, the displacement turns out to be: d = $V_b T_X$ (and is thus proportional to the number of transmitted cycles). Afterward, the bubble is dragged again along the (vertical) direction of the fluid flow. The (1) was solved numerically using a simple Euler one-step method.

III. Results and Discussions

The translation of the bubbles in the wave propagation direction was investigated following two different approaches. In a first set of measurements, the influence of US parameters such as the pulse length and the peak acoustic pressure were studied for specific bubble diameters. Second, the displacement induced by the radiation force was examined as a function of the bubbles' diameter and density (defined by the separation distance between two successive bubbles). Air bubbles with a diameter between 35 μm to 79 μm were studied. Their rising velocity (i.e., the fluid velocity) ranged from 200 μm/ms to 290 μm/ms. The bubble maker was arranged to guarantee that, in the measurement region, the bubble velocity was equal to the fluid velocity. Fig. 2 shows an example of the translational displacement produced by a single acoustic pulse composed of 10 cycles and generating an acoustic pressure of 110 kPa. Three subsequent frames spaced 1 ms apart (one taken before and two after the US pulse transmission) are overlapped in the same picture. The resting diameter of the bubbles was 48 μm. X_{initial} represents the position of the bubbles before insonification and Δ is the

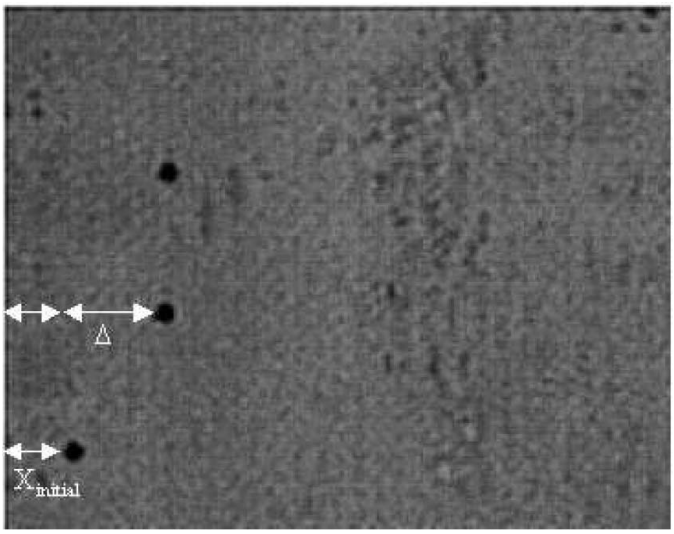

Fig. 2. Superposition of three consecutive frames showing the displacement of a 48 μm bubble induced by a 10-cycle US pulse emitting 110 kPa at 130 kHz. (a) Before the US burst, (b) and (c) after the US burst. The vertical displacement corresponds to the 260 μm/ms fluid velocity.

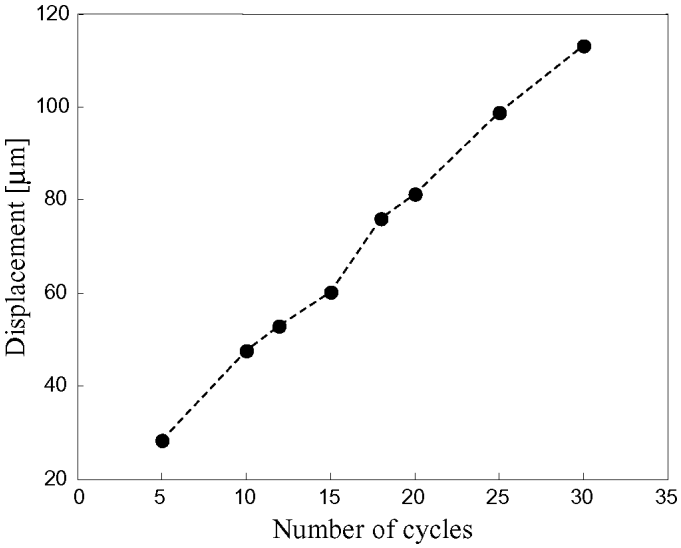

Fig. 3. Measured displacements for 48 μm bubbles as a function of the pulse length.

measured displacement. It can be observed that the bubble is displaced to the right by an amount of about 165 μm and has moved up about 250 μm. The horizontal translation is consistent with the prediction of the model, and the vertical movement of the bubble is associated to the drag force of the fluid (Archimede's force being negligible).

Fig. 3 displays the measured displacement as a function of the pulse length. The number of cycles ranged from 5 to 30. The diameter of the bubbles was 48 μm and the acoustic pressure was set at 54 kPa. As expected from the theory, the displacement increases linearly with the number of cycles. Fig. 4 displays the influence of the transmitted acoustic pressure on three different bubble sizes:

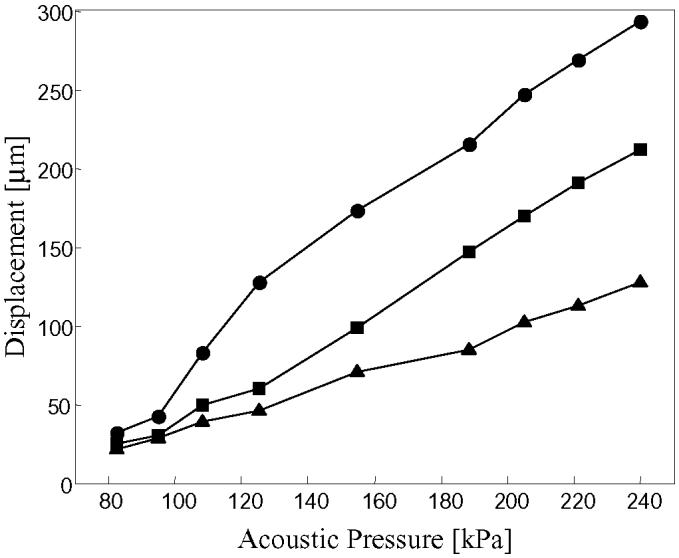

Fig. 4. Measured displacements as a function of the transmitted acoustic pressure for three different bubble diameters: 48 μm (circle), 55 μm (square) and 62 μm (triangle).

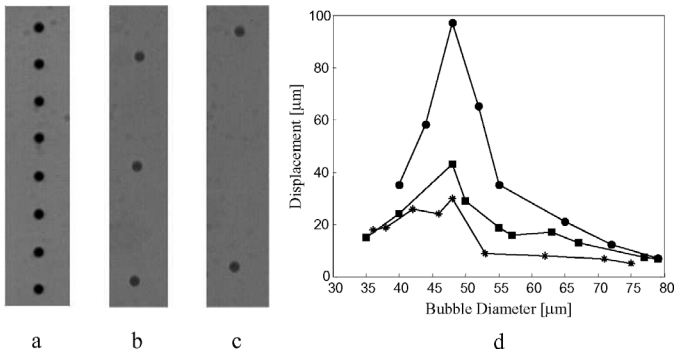

Fig. 5. Bubble patterns with separation distances between two successive bubbles of: (a) 200 μm, (b) 350 μm, and (c) 900 μm. (d) Bubble displacements as function of diameter for three different separation distances between two successive bubbles: 900 μm (•), 350 μm (■), and 200 μm (*).

62 μm (triangle), 55 μm (square), and 48 μm (circle). The bubbles were insonified with a 10-cycle burst, and the distance between two successive bubbles was kept at about 1 mm. In all cases, according to the theoretical model, the combined action of radiation and drag force should produce a displacement that varies quasilinearly with the acoustic pressure. This linear dependency between the displacement and the acoustic pressure can be noticed for the three bubble diameters, although in the case of a resonant bubble 48 μm, the growing rate differs at low and high acoustic pressure levels. We also can observe that each curve exhibits a different slope. As the bubble is closer to the resonance size 48 μm, the measured displacement increases with acoustic pressure at a much faster rate. Although the three bubble diameters experience quite similar displacements at low pressure, the difference is dominant at high-pressure levels. For instance, the difference between translations of 48 μm and 62 μm bubbles is only 10 μm at 48 kPa, but reaches 170 μm at 120 kPa.

In a second set of experiments, the influence of the bubble density was investigated by exploiting the bubble maker capability of generating bubbles with various mutual distances. Fig. 5(a)–(c) show 48 μm bubbles with three different distributions, corresponding to separation distances around (a) 200 μm, (b) 350 μm, and (c) 900 μm, respectively. The displacement measured for each distribution is displayed in Fig. 5(d) as a function of the bubble diameter. The US burst consisted of 10 cycles yielding to a peak acoustic pressure of 54 kPa. We can first observe that the change in the measured displacement depends on the bubble size. Each curve exhibits a maximum for a bubble diameter of 48 μm, which corresponds to the resonance size for a transmit frequency of 130 kHz. When the bubbles are smaller or larger than the resonance size, the displacement rapidly decreases. It also can be noticed that the measured displacement is highly dependent on the density of the bubbles. When the separation distance between two successive bubbles decreases, the displacement induced by the US pulse is considerably reduced. The effect is dominant for bubbles around the resonance size, and the difference gets smaller for bubbles larger or smaller than the resonance size. In the case of resonant bubbles, the displacement is reduced by 56% when the separation distance between two bubbles goes down from 900 μm to 350 μm and by 70% when the separation distance is reduced to 200 μm. As the separation distance decreases, the displacement for bubbles larger than the resonance size exhibit a smaller decay. Considering the smallest distance between the bubbles, the displacement for bubbles of 53 μm and 75 μm decays only by a factor of 2, but this decay reaches a factor of 4 for the largest separation distance. This set of measurements underlines the fact that there is a strong interaction between the bubbles when they get closer to each other. Only for large separation distances (e.g., $>$ 900 μm), each bubble can be considered as an independent scatterer. When the number of bubbles increases, each bubble interferes with its neighboring bubbles. This interaction is mainly influenced by the secondary radiation force resulting from the pulsating bubbles. The secondary radiation force between bubbles arises when a pulsating bubble is radiating a pressure field acting on a second bubble. When bubbles with a similar diameter are considered, the secondary radiation force results in an attractive force. Therefore, it may conduct to a bubble streamline more resistant to the primary radiation force. An example of the effect of the secondary radiation force is given in Fig. 6. The resting radius of the bubbles is 53 μm and the separation distance is 170 μm, as shown in Fig. 6(a). When a single pulse with an acoustic pressure of 110 kPa is applied to the bubbles, the bubbles' flow pattern is disturbed, and the bubbles get closer as visible in Fig. 6(b). The measured displacement was compared to the displacement computed from the theoretical model as a function of the bubble size.

Fig. 7 shows the simulated (circle) and experimental displacements (diamond) as a function of the bubble di-

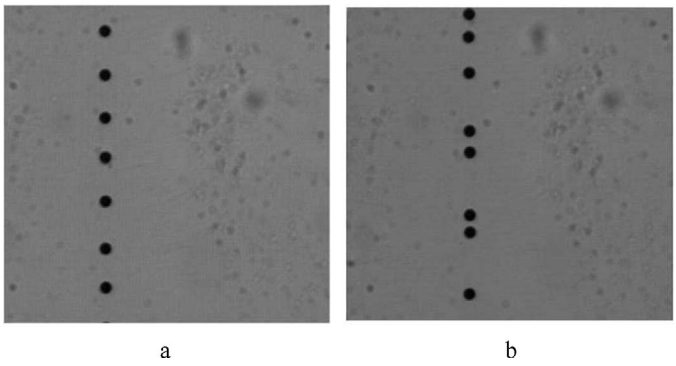

Fig. 6. Example of the secondary radiation force effect on a streamline of microbubbles. (a) Before the US burst. (b) After the US burst.

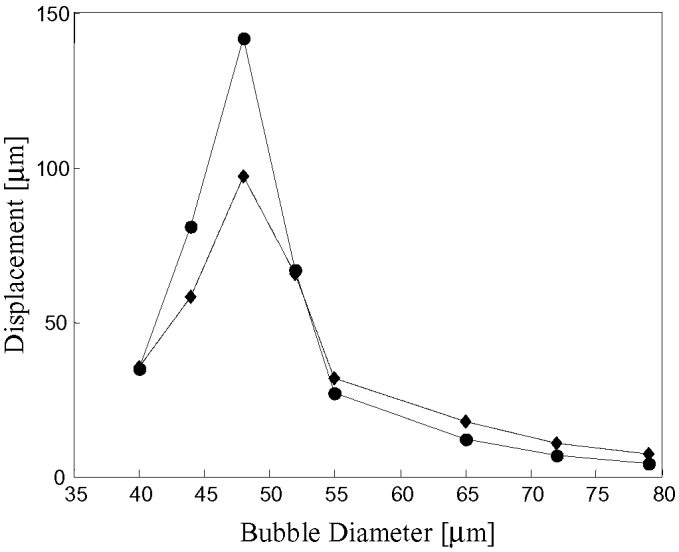

Fig. 7. Comparison between computed (circle) and measured (diamond) bubble displacements at 55 kPa with a separation distance of 900 μm as a function of bubble diameter.

ameter. Because the theoretical model considers the behavior of a single bubble, the largest separation distance between the bubbles was maintained in these experiments. A burst of 10 cycles with a pressure of 54 kPa was applied to the bubbles. Both curves present the same tendency: a maximal displacement is observed at the resonance size. For bubbles far above the resonance size, the theoretical model agrees quite well with the experiments. The difference between both displacements varies about 15%. Larger discrepancy can be observed around the resonance size, at which the simulations overestimated the displacement of the bubbles by about 40%. The discrepancy between theory and measurements for resonant bubbles might be ascribed partly to measurement uncertainties and partly to an inadequate theoretical description of the bubble oscillations. Due to the strongly resonant behavior of the bubbles, a possible small difference between the measured and the actual bubble size can dramatically influence the results. Such problems were limited, although not totally eliminated, by changing the bubble diameter until a maximal displacement could be observed. Moreover, resonating free air bubbles experience very strong nonlinear expansions and contractions. And the model considers a fixed (resting) radius for the drag force and ignores possible contribution of added mass force, which is known to be relevant for highly nonlinear oscillations [10]. The discrepancies between measurements and model predictions become more evident at higher pressures. In fact, the model assumes that the bubble remains spherical under ultrasonic irradiation. However, for resonant bubbles, and relatively high pressures, such an assumption no longer is valid. This finding was recently demonstrated by using the ultra fast digital camera developed in our laboratory named Brandaris [11], which can acquire up to 128 frames at a maximal frame rate of 25 MHz. As an example, the oscillations yielded by a 60 kPa pressure in a bubble with 44 μm resting radius were recorded at a frame rate of 1.5 MHz and are documented in Fig. 8. This figure shows various frames taken during a single 6-cycle insonation burst. The first three frames show the bubble at rest [Fig. 8(a)], at maximal compression [Fig. 8(b)], and at maximal expansion [Fig. 8(c)]. Fig. 8 (d)–(f), taken during later insonation cycles, clearly display nonspherical oscillations of the bubbles. The effect was reversible; and, after the passage of the US burst, the bubbles recovered their initial diameter and shape. Such images confirm that, even at a relatively low acoustic pressure, the bubble shape does not remain spherical and new surface vibration modes are generated.

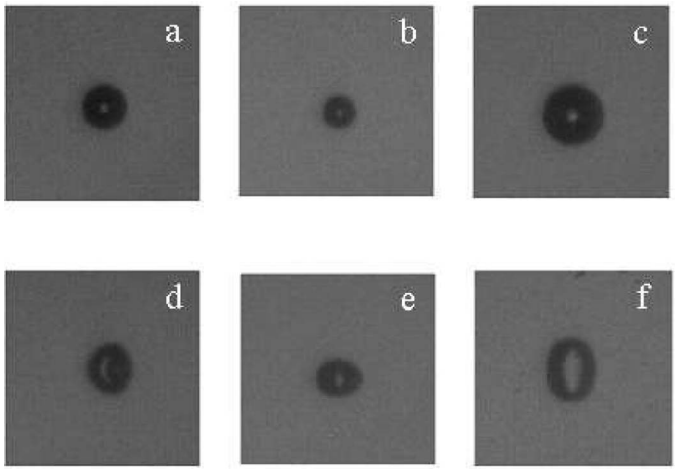

Fig. 8. Oscillations of a bubble with 44 μm diameter observed with the Brandaris 128. (a)–(c) Nonlinear bubble pulsations. (d)–(f) Nonspherical bubble vibrations.

IV. Conclusions

In this paper, the effects of the acoustic radiation force on the bubble translation were investigated as a function of the bubble characteristics and the US parameters. As expected by theory, the bubble displacement increases linearly with both the burst length and the transmitted acoustic pressure. The displacement is strongly correlated

to the bubble diameter as well as to the separation distance between two bubbles. It has been demonstrated that, independently of the US settings, bubbles at the resonance size lead to a maximal displacement, and other bubble sizes produce lower but nonnegligible displacements. The number density of the bubbles also considerably affects the measured displacement. For high bubble concentration, the displacement induced by the US force strongly decreases. This may be related to the effect of secondary radiation force, which seems to have a limiting effect similar to that of the drag force. The theoretical model agrees quite well with the experimental measurements, both qualitatively and quantitatively. Only around the resonance size, the simulations appreciably overestimate the displacement. Such disagreement was not found when the model was applied to US contrast agents with diameters in the range of a few microns [3]. This is probably due to the fact that the model neglects the bubble size oscillations—which for contrast agents may be limited due to the encapsulating shell—but are relevant in the case of large, free air bubbles like those used in this work. At relatively high-pressure levels, the behavior of free air bubbles is quite complex, as observed with an ultra fast digital camera. Therefore, the simplified theoretical model may not be accurate enough. A more complex model, including the effect of bubble oscillations on the drag force as well as the added mass force, would be more suitable in this regime. Overall, this study has demonstrated that even a single US pulse may disturb considerably a flow path of individual air bubbles.

Acknowledgments

The authors would like to acknowledge Massimo Corsi, Florence, Italy, for valuable help in simulation work.

References

[1] V. Bjerknes, *Fields of Force*. New York: Columbia Univ. Press, 1906.

[2] J. Smith, D. Evans, and A. Naylor, "Analysis of the frequency modulation present in Doppler ultrasound signals may allow differentiation between particulate and gaseous cerebral emboli," *Ultrasound Med. Biol.*, vol. 23, no. 5, pp. 727–734, 1997.

[3] P. Dayton, K. Morgan, A. Klibanov, G. Brandenburger, K. Nightingale, and K. Ferrara, "A preliminary evaluation of the effects of primary and secondary radiation forces on acoustic contrast agents," *IEEE Trans. Ultrason., Ferroelect., Freq. Contr.*, vol. 44, no. 6, pp. 1264–1277, 1997.

[4] P. Tortoli, M. Pratesi, and V. Michelassi, "Doppler spectra from contrast agents crossing an ultrasound field," *IEEE Trans. Ultrason., Ferroelect., Freq. Contr.*, vol. 47, no. 3, pp. 716–726, 2000.

[5] P. Tortoli, V. Michelassi, M. Corsi, D. Righi, and Y. Takeushi, "On the interaction between ultrasound and contrast agents during Doppler investigations," *Ultrasound Med. Biol.*, vol. 27, no. 9, pp. 1265–1273, 2001.

[6] P. Dayton, J. Allen, and K. Ferrara, "The magnitude of radiation force on ultrasound contrast agents," *J. Acoust. Soc. Amer.*, vol. 112, no. 5, pp. 2183–2192, 2002.

[7] P. Palanchon, J. Klein, and N. de Jong, "Production of standardized air bubbles: Application to embolism studies," *Rev. Sci. Instrum.*, vol. 74, no. 4, pp. 2558–2564, 2003.

[8] T. Leighton, *The Acoustic Bubble*. London: Academic, 1994.

[9] H. Medwin, "Counting bubbles acoustically: A review," *Ultrasonics*, vol. 15, no. 1, pp. 7–13, 1977.

[10] T. Matula, "Bubble levitation and translation under single bubble sonoluminescence conditions," *J. Acoust. Soc. Amer.*, vol. 114, no. 2, pp. 775–781, 2003.

[11] C. Chin, C. Lancée, J. Borsboom, F. Mastik, M. Frijlink, M. Versluis, D. Lhose, and N. de Jong, "Brandaris 128: A digital 25 million frames per second camera with 128 highly sensitive frames," *Rev. Sci. Instrum.*, vol. 74, no. 12, pp. 5026–5034, 2003.

Peggy Palanchon was born in France, in 1973. She earned a master's degree in mechanics and physics in 1996 from the Pierre et Marie Curie University (Paris VI), Paris, France. In 1998, she joined the Whitaker Center, State College, PA, where she worked for 1 year.

Her research project consisted of modeling and fabricating novel transducers for medical applications, particularly Doppler applications. In July 1999, she joined the Department of Experimental Echocardiography of the Thoraxcentre, Erasmus MC in Rotterdam, The Netherlands, to pursue her Ph.D. degree Her research interests include ultrasound volume measurement, microemboli detection, and Doppler ultrasound.

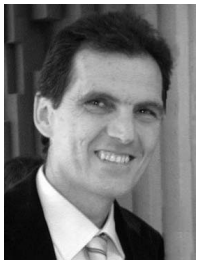

Piero Tortoli (M'91–SM'96) was born in Florence, Italy, in 1953. He received the Laurea degree in electronic engineering in 1978. Since then, he has been with the Electronic Engineering Department of the University of Florence, Italy, where he is a full professor of electronics.

His main interests are in the area of signal processing systems and devices with application to biomedical instrumentation and radar. Since 1981, he has been involved in research on ultrasonics with emphasis on Doppler techniques.

Professor Tortoli has authored or coauthored over 100 scientific papers in international journals and conference proceedings. He is on the Editorial Board of *Ultrasound in Medicine and Biology*. He has been a member of the Technical Program Committee of international conferences and workshops, including the IEEE International Ultrasonics Symposium. He has served as Chair of the 22nd International Symposium on Acoustical Imaging (1995), co-Chair of the 1998 ICB Seminar on Ultrasound in Biomeasurements, Diagnostics, and Therapy, and Chair of the 12th New England Doppler Conference (2003).

Ayache Bouakaz graduated from the University of Sétif, Algeria, from the Department of Electrical Engineering. He obtained his Ph.D. degree in 1996 from the Department of Electrical Engineering at the University of INSA (Institut National des Sciences Appliquées), Lyon, France.

In 1998 he joined the Department of Bioengineering at Penn State University in State College, PA, where he worked as a postdoc for 1 year. Since February 1999, he has been employed at the Erasmus University Medical Center, Rotterdam, The Netherlands. His research focuses on imaging, ultrasound contrast agents, transducer design, and drug delivery.

Michel Versluis was born in the Netherlands in 1963. He graduated in Physics in 1988 from the University of Nijmegen, the Netherlands, with a special interest in Molecular Physics and Astrophysics, working in the field of far-infrared laser spectroscopy of interstellar molecular species. Later, he specialized in the application of intense tunable UV lasers for flame diagnostics resulting in a successful defense of his Ph.D. thesis in 1992. After a two year research position working on molecular dynamics at Griffith University, Brisbane, Australia, he continued to work on developing laser diagnostic techniques for internal combustion engines (Lund, Sweden) and industrial jet flames and solid rocket propellants (Delft, The Netherlands). Michel Versluis is now a lecturer at the University of Twente, the Netherlands, in the Physics of Fluids group working on the experimental study of bubbles and jets in multiphase flows and granular flows. He also works on the use of microbubbles as tools for medical diagnosis and therapy.

Nico de Jong (A'97) was born in 1954. He graduated from Delft University of Technology, Delft, The Netherlands, in 1978. He received his M.Sc. degree in the field of pattern recognition.

Since 1980, he has been a staff member of the Thoraxcentre of the Erasmus University Medical Center, Rotterdam, The Netherlands. At the Department of Biomedical Engineering, he developed linear and phased array ultrasonic probes for medical diagnosis, especially compound and transesophageal transducers. In 1986 his interest in ultrasound applications shifted toward the theoretical and practical background of ultrasound contrast agents. In 1993 he received his Ph.D. degree for "Acoustic Properties of Ultrasound Contrast Agents."

Currently he is interested in the development of 3-D transducers and a fast framing camera system. Dr. de Jong is the project leader of Stichting voor de Technisch Wetenschappen (STW) and Stichting voor Fundamenteel Onderzoek der Materie (FOM) projects on ultrasound contrast imaging and drug delivery systems. Together with Folkert ten Cate, M.D., he is organizer of the annual European Symposium on Ultrasound Contrast Imaging, held in Rotterdam and attended by approximately 175 scientists from all over the world.